Polyhedron 29 (2010) 2311–2317

Contents lists available at ScienceDirect

Polyhedron

journal homepage: www.elsevier.com/locate/poly

Synthesis, spectral characterization and electrochemical properties of (2-alkylthiobenzoyl)ferrocenes. Crystal structures of 2-methylthio, 2-ethylthio and 2-isopropylthio derivatives

Zoran Ratković [a], Slađana B. Novaković [b], Goran A. Bogdanović [b], Dejan Šegan [c], Rastko D. Vukićević [a,*]

[a] Department of Chemistry, Faculty of Science, University of Kragujevac, R. Domanovića 12, 34000 Kragujevac, Republic of Serbia
[b] Vinča Institute of Nuclear Sciences, Laboratory of Theoretical Physics and Condensed Matter Physics, P.O. Box 522, 11001 Belgrade, Republic of Serbia
[c] Faculty of Chemistry, University of Belgrade, P.O. Box 158, 11001 Belgrade, Republic of Serbia

ARTICLE INFO

Article history:
Received 27 March 2010
Accepted 30 April 2010
Available online 23 May 2010

Keywords:
Ferrocene
2-Alkylthiobenzoic acids
(2-Alkylthiobenzoyl)ferrocenes
Cyclic voltammetry
Crystal structure
C–H. . .π interactions

ABSTRACT

The one-pot synthesis of seven new (2-alkylthiobenzoyl)ferrocenes has been achieved by Friedel–Crafts acylation of ferrocene with acid chlorides generated *in situ* from the corresponding carboxylic acids and phosphorous trichloride. The obtained compounds were characterized by spectroscopic data (UV, IR, ^{1}H and ^{13}C NMR), whereas their electrochemical properties have been investigated by cyclic voltammetry. The single-crystal X-ray structure determinations for three of them are also reported. Each of the three derivatives exhibits the intramolecular C–H. . .O interaction which involves the donor from the cyclopentadienyl (Cp) ring and the carbonyl oxygen as acceptor. This interaction favors the coplanar arrangement of the two moieties. The angles between the vectors coinciding the C–O bonds and the corresponding Cp planes are all below 6.4°. Conventional hydrogen bonds do not exist in any of the three crystal structures but some weak intermolecular interactions of the C–H. . .O, C–H. . .S and C–H. . .π types have been found and analyzed in detail. Different geometrical parameters for these crystal structures as well as for 22 similar ones extracted from Cambridge Structural Database (CSD) have been compared and analyzed.

1. Introduction

There is no other example among unnatural compounds that has captured the attention of chemists so intensively as ferrocene and its derivatives. It is the consequence of several unique features of ferrocenes. First of all, ferrocene itself is a commercially available and relatively cheap compound which could be easily functionalized to derivatives that are very appreciated for their outstanding stability in both aqueous and non-aqueous media. The iron core of ferrocenes is able to exist in both Fe^{2+} or Fe^{3+} making them to possess very interesting redox properties. Ferrocenes have applications in numerous fields, particularly in those such as organic synthesis, catalysis, electrochemical, electronic absorption and nonlinear optical materials [1,2]. Although the earliest attempts to apply ferrocene derivatives in medicine were discouraging [3,4], chemists did not abandon this idea, and nowadays many ferrocene derivatives have been biologically evaluated against certain diseases. These investigations have showed that many ferrocenyl compounds display interesting cytotoxic, antitumor, antimalarial, and antimicrobial activity [5–14].

The most frequently used method in functionalization of ferrocene is Friedel–Crafts acylation, discovered by Woodward at the early days of ferrocene [15]. The products of this reaction, the corresponding ferrocenyl ketones, are also known as the compounds which are susceptible to many easily achievable transformations. Their carbonyl group allows for introducing of heteroatoms like nitrogen, sulfur or phosphorus in the form of a certain nucleophilic functional group. It is particularly useful to introduce an additional heteroatom in the same time when acylating ferrocene, using acyl halides containing the corresponding functional groups. This methodology is, however, limited by the fact that nucleophilic functional groups form complexes with Lewis acids preventing thus the necessary acylating complex formation. Several years ago we improved above mentioned Woodward's acylation of ferrocene and showed that both carboxylic acid chlorides and the Lewis catalyst can be generated *in situ*, making, thus, the synthesis of acylferrocenes much shorter [16–18]. Following this procedure we recently prepared and characterized several acylferrocenes containing sulfur in the side chain [19]. The present paper deals with the continuation of these investigations, and we wish to report herein on the synthesis of seven new (2-alkylthio)benzoylferrocenes (**1a–g**, Fig. 1). The distance between the carbonyl group and the sulfur atom in these bifunctional molecules makes them

---

* Corresponding author. Tel.: +381 34 300 268; fax: +381 34 335 040.
E-mail address: vuk@kg.ac.rs (R.D. Vukićević).

0277-5387/$ - see front matter © 2010 Elsevier Ltd. All rights reserved.
doi:10.1016/j.poly.2010.04.034

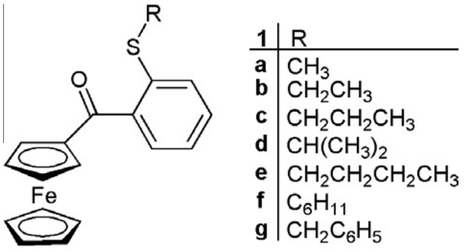

1a-g

Fig. 1. (2-alkylthiobenzoyl)ferrocenes.

interesting for different synthetic purposes, particularly as a potential starting material for synthesis of bidentate sulfur containing ligands.

The synthesis of ketones **1a–g** has been achieved by introducing at once both the carbonyl group and sulfur atom into the target molecule. The obtained compounds are well characterized by spectral data and cyclovoltammetric measurements, whereas single-crystal X-ray structure determinations for three of them (**1a**, **b**, and **d**) are also performed.

2. Experimental

2.1. General

All chemicals were commercially available and used as received, except that the solvents were purified by distillation. *S*-Alkylthiosalicylic acids were synthesized by alkylation of thiosalicylic acid (Merck), following the procedure described elsewhere [20]. Chromatographic separations were carried out using silica gel 60 (Merck, 230–400 mesh ASTM), whereas silica gel 60 on Al plates, layer thickness 0.2 mm (Merck), was used for TLC. IR spectra were recorded on Perkin–Elmer Spectrum One FT-IR spectrometer with a KBr disc. UV measurements were performed on a Perkin–Elmer Lambda 35 double-beam UV–Vis spectrophotometer in CH_2Cl_2 as the solvent. NMR spectra were recorded on a Varian Gemini (200 MHz) spectrometer, using $CDCl_3$ as the solvent and TMS as the internal standard. Chemical shifts are expressed in δ (ppm). Electrochemical measurements were performed by using a CH Instruments (Austin, TX) potentiostat CHI760b Electrochemical Workstation. A standard three-electrode cell (5 mL) equipped with a platinum disk (d = 2 mm), a platinum wire and a silver wire immersed in 0.1 M $LiClO_4$ solution in CH_3CN as the working, counter and reference electrode, respectively.

2.2. General procedure for the synthesis of compounds *1a–g*

The solution of the corresponding carboxylic acid **3a–g** (1 mmol), ferrocene (186 mg, 1 mmol) and PCl_3 (~0.1 mL, 1 mmol,) in 50 mL of CH_2Cl_2 was stirred overnight at room temperature in a two necked round-bottom bottle, supplied with a reflux condenser protected from air moisture with the $CaCl_2$ tube. Anhydrous $AlCl_3$ (200 mg, 1.5 mmol) was added to this mixture which immediately become dark-violet, and stirring was continued for additional 4 h. The resulting mixture was then poured into a cold KOH solution (50 mL, 1 mol/L). The red–orange organic layer was separated whereas the aqueous one was extracted with an additional portion of CH_2Cl_2 (30 mL). The collected organic layers were washed with water, brine and water successively. After drying over anhydrous Na_2SO_4, the solvent was evaporated, and the residue was purified by column chromatography (SiO_2/light petroleum, then toluene or toluene/ethyl acetate 9:1). The first fraction (light yellow) was unconsumed ferrocene and second one (orange or red) was the corresponding ketone. After evaporation of the solvent, remains colored oil which solidified after standing to deep red–orange solids (except in the case of **1c**).

2.2.1. (2-Methylthiobenzoyl)ferrocene (*1a*)

65%; m.p. 95–96 °C; red crystals; IR (KBr): ν = 3061, 2921, 2648, 1674, 1562, 1463, 1412, 1317, 1272, 1255, 1062, 1046, 897, 743, 711, 694, 652 and 551 cm^{-1}; ^1H NMR (200 MHz, $CDCl_3$): δ = 2.45 (s, 3H), 4.29 (s, 5H), 4.56 (t, 2H, J = 1.78 Hz), 4.79 (t, 2H, J = 1.78 Hz,), 7.17 (m, 1H), 7.33–7.43 (m, 2H) and 7.59 ppm (m, 2H); ^{13}C NMR (200 MHz, $CDCl_3$): δ = 16.3, 69.8, 71.2, 72.5, 78.6, 123.7, 126.4, 128.3, 130.4, 138.3, 138.6 and 199.5 ppm.

2.2.2. (2-Ethylthiobenzoyl)ferrocene (*1b*)

53%; m.p. 103–104 °C; red crystals; IR (KBr): ν = 3092, 2967, 2922, 1642, 1582, 1444, 1374, 1294, 1255, 1041, 1030, 856, 756, 700, 694, 652 and 498 cm^{-1}; ^1H NMR (200 MHz, $CDCl_3$): δ = 1.29, (t, 3H, J = 7.34 Hz), 2.94 (q, 2H, J = 7.34 Hz,), 4.29 (s, 5H), 4.55 (t, 2H, J = 1.93 Hz), 4.77 (t, 2H, J = 1.94 Hz), 7.17–7.42 (m, 3H), and 7.52–7.57 ppm (m, 1H); ^{13}C NMR (200 MHz, $CDCl_3$): δ = 13.8, 27.7, 69.9, 71.1, 72.5, 78.8, 124.5, 128.2, 128.6, 130.1, 136.1, 140.4 and 199.9 ppm.

2.2.3. (2-Propylthiobenzoyl)ferrocene (*1c*)

25%; red–orange oil; IR (KBr): ν = 3434, 3110, 2961, 2927, 1639, 1584, 1462, 1442, 1399, 1292, 1042, 855, 824, 747 and 488 cm^{-1}; ^1H NMR (200 MHz, $CDCl_3$): δ = 0.99 (t, 3H, J = 7.3 Hz,), 1.66 (hx, 2H, J = 7.3 Hz,), 2.89 (t, 2H, J = 7.3 Hz,), 4.29 (s, 5H), 4.55 (t, 2H, J = 2 Hz), 4.77 (t, 2H, J = 2 Hz), 7.2–7.24 (m, 1H), 7.38–7.42 (m, 2H) and 7.52–7.56 ppm (m, 1H); ^{13}C NMR (200 MHz, $CDCl_3$): δ = 13.5, 22.1, 35.7, 69.9, 71.1, 72.5, 78.9, 124.4, 128.2, 128.7, 130.1, 136.4, 140.4 and 199.9 ppm.

2.2.4. (2-Isopropylthiobenzoyl)ferrocene (*1d*)

40%; m.p. 80–81 °C; red crystals; IR (KBr): ν = 3095, 2962, 2924, 1642, 1584, 1462, 1442, 1375, 1292, 1106, 1041, 1003, 850, 824, 749, 704, 657 and 486 cm^{-1}; ^1H NMR (200 MHz, $CDCl_3$): δ = 1.26 (d, 6H, J = 6.7 Hz), 3.45 (h, 1H, J = 6.7 Hz), 4.29 (s, 5H), 4.54 (t, 2H, J = 1.97 Hz), 4.73 (t, 2H, J = 1.97 Hz) and 7.24–7.54 ppm (m, 4H); ^{13}C NMR (200 MHz, $CDCl_3$): δ = 22.8, 37.8, 69.8, 71, 72.4, 78.9, 125.2, 127.8, 129.8, 131.1, 134.6, 142.0 and 200.2 ppm.

2.2.5. (2-Butylthiobenzoyl)ferrocene (*1e*)

26%; m.p. 65–66 °C; red–orange crystals; IR (KBr): ν = 2956, 2928, 1639, 1584, 1463, 1442, 1375, 1292, 1106, 1041, 1003, 855, 824, 749, 703, 667 and 486 cm^{-1}; ^1H NMR (200 MHz, $CDCl_3$): δ = 0.88 (t, 3H, J = 7.32 Hz), 1.37–1.71 (m, 4H), 2.91 (t, 2H, J = 7.31 Hz), 4.29 (s, 5H), 4.55 (t, 2H, J = 1.95 Hz), 4.77 (t, 2H, J = 1.95 Hz), 7.18–7.41 (m, 3H) and 7.51–7.55 ppm (m, 1H); ^{13}C NMR (200 MHz, $CDCl_3$): δ = 13.5, 21.9, 30.7, 33.2, 69.8, 71.1, 72.5, 78.8, 124.2, 128.1, 128.3, 130.1, 136.5, 140.0 and 199.8 ppm.

2.2.6. (2-Cyclohexylthiobenzoyl)ferrocene (*1f*)

22%; m.p. 92 °C; red–orange crystals; IR (KBr): ν = 2926, 2851, 1639, 1583, 1443, 1374, 1290, 1262, 1176, 1106, 1040, 998, 854, 822, 750, 702, 656 and 483 cm^{-1}; ^1H NMR (200 MHz, $CDCl_3$): δ = 1.15–2.05 (m, 10H), 3.18 (m, 1H), 4.28 (s, 5H), 4.55 (t, 2H, J = 1.97 Hz), 4.72 (t, 2H, J = 1.97 Hz) and 7.24–7.53 ppm (m, 4H); ^{13}C NMR (200 MHz, $CDCl_3$): δ = 25.6, 26.0, 33.1, 46.4, 69.9, 71.1, 72.5, 79.1, 125.3, 127.9, 129.7, 131.3, 134.1, 142.3 and 200.4 ppm; *Anal.* Calc. for $C_{23}H_{24}FeOS$ (404.35): C, 68.32; H, 5.98; Fe, 13.81; O, 3.96; S, 7.93. Found: C, 68.31; H, 5.97%.

2.2.7. (2-Benzylthiobenzoyl)ferrocene (*1g*)

20%; m.p. 118–119 °C; red–orange crystals; IR (KBr): ν = 2922, 2852, 1636, 1583, 1494, 1441, 1374, 1292, 1176, 1106, 1041, 1026, 854, 825, 748, 701, 656 and 484 cm^{-1}; ^{1}H NMR (200 MHz, $CDCl_3$): δ = 4.12 (s, 2H), 4.28 (s, 5H), 4.55 (t, 2H, J = 1.96 Hz), 4.75 (t, 2H, J = 1.97 Hz), 7.12–7.45 (m, 3H) and 7.53–7.58 ppm (m, 1H); ^{13}C NMR (200 MHz, $CDCl_3$): δ = 38.9, 69.9, 71.1, 72.5, 78.8, 125.1, 127.1, 128.2, 128.4, 129, 129.8, 130.1, 135.6, 136.9, 140.7 and 199.9 ppm; *Anal.* Calc. for $C_{24}H_{20}FeOS$ (412.32): C, 69.91; H, 4.89; Fe, 13.54; O, 3.88; S, 7.78. Found: C, 69.87; H, 4.93%.

2.3. X-ray data collection and structure refinement for compounds 1a, 1b and 1d

Crystal data and experimental details for the three ferrocene derivatives are summarized in Table 1. The diffraction data were collected on an Enraf–Nonius CAD4 diffractometer [21] by using graphite-monochromated Mo Kα (0.71073 Å) radiation at 293(2) K. The data were corrected for Lorentz and polarization effects [22]. Crystal structures were solved by direct methods with the program SHELXS97 [23a] and refined on the F^2 by full-matrix least-square method with SHELXL97 [23b] both incorporated in WINGX [24] program package.

All H atoms were placed at geometrically calculated positions with the C–H distances fixed to 0.93 from Csp^2 and 0.96, 0.97 and 0.98 Å from methyl, methylene and methine Csp^3, respectively. The corresponding isotropic displacement parameters of the hydrogen atoms were equal to 1.2 U_{eq} and 1.5 U_{eq} of the parent Csp^2 and Csp^3, respectively. The software used for the preparation of the materials for publication: PLATON [25], PARST [26] and ORTEPIII [27].

Table 1
Crystallographic data for **1a**, **1b** and **1d**.

	1a	1b	1d
Empirical formula	$C_{18}H_{16}FeOS$	$C_{19}H_{18}FeOS$	$C_{20}H_{20}FeOS$
Formula weight	336.22	350.26	363.26
Color	deep red	deep red	deep red
T (K)	293(2)	293(2)	293(2)
Crystal size (mm)	0.25 × 0.14 × 0.10	0.33 × 0.20 × 0.15	0.28 × 0.18 × 0.12
Crystal system	monoclinic	monoclinic	monoclinic
Space group	$P2_1$	$C2/c$	$P2_1/c$
Lattice constants			
a (Å)	7.7062(13)	25.323(12)	11.694(9)
b (Å)	12.624(4)	7.767(5)	10.274(3)
c (Å)	8.063(2)	20.315(11)	15.068(12)
α (°)	90.00	90.00	90.00
β (°)	102.37(2)	124.56(4)	105.18(5)
γ (°)	90.00	90.00	90.00
Volume (Å^3)	766.2(3)	3291(3)	1741(14)
Z	2	8	4
D_{calc}, ρ (g cm^{-3})	1.457	1.414	1.386
θ range for data collection (°)	2.59–27.97	1.95–25.98	1.81–25.97
Absorption coefficient (mm^{-1})	1.115	1.042	0.987
F(0 0 0)	348	700	756
Reflections collected	1739	5567	3583
Independent reflections	1623	3031	3451
Parameters	187	199	208
Goodness-of-fit (GOF)	0.985	1.008	0.938
R_1 [$I > 2\sigma(I)$]	0.0400	0.0371	0.0517

3. Results and discussion

3.1. Synthesis

Present investigations we started by submitting ferrocene to the reaction with an equimolar mixture of thiosalicylic (2-mercaptobenzoic) acid (**2**) and phosphorus trichloride in the presence of aluminum trichloride. Encouraged by our earlier finding that salicylic acid can be used in a one-pot synthesis of (2-hydroxybenzoyl)ferrocene [18,28], we expected to obtain (2-mercaptobenzoyl)ferrocene. However, the reaction failed to give the desired product, and we decided to continue the investigations by *S*-alkylation of acid **2** (Scheme 1), hoping that the alkylthio group will not hinder the reaction, in contrast to the unprotected SH group. Applying the known procedure [20], we obtained the corresponding *S*-alkylthiosalicylic acids **3a–g** and, then, submitted them to the reaction with phosphorus trichloride. The obtained intermediate chlorides (**4a–g**) have not been isolated and purified, but treated *in situ* with aluminum trichloride and ferrocene resulting in the corresponding sulfur containing ferrocenyl ketones **1a–g** (20–65%; Scheme 1).

3.2. Spectral characterization

NMR and IR spectral data of the synthesized new compounds **1a–g** clearly confirm their structures. Thus, the IR spectra of all compounds contain the intensive bond at 1636–1642 cm^{-1}, which is attributed to the carbonyl group. On the other hand, in ^{1}H NMR spectra of all compounds three signals appear at the same position – at 4.29 (s), 4.55 (t) and 4.80 (t) ppm. They correspond to the five protons of unsubstituted cyclopentadienyl ring and two proton pairs of monosubstituted cyclopentadienyl ring, respectively. All these spectra also contain multiple signals at 7.17–7.60 ppm, corresponding to the four protons of an *ortho*-disubstituted benzene ring. The multiplicity and the intensity of other signals appearing in these spectra exactly depict the specific structures of the corresponding compounds.

The common signals in all ^{13}C NMR spectra belong to the carbons of unsubstituted cyclopentadienyl ring (at 70.0 ppm), two methylene carbon pairs of monosubstituted cyclopentadienyl ring (at 71.50 and 72.6 ppm), one quaternary carbon atom of the same ring (at 78.80 ppm) and one carbonyl carbon (at 200 ppm). The signals of the phenyl carbons of all the compounds, however, differ slightly but noticeably.

All synthesized compounds **1a–g** in UV spectra exhibit absorption maximum at almost the same wave length (about 475 nm) as it is showed by Fig. 2.

3.3. Molecular geometry and intermolecular interactions in the crystal structures of compounds 1a, 1b and 1d

With the aim to compare the geometrical features of compounds **1a, 1b** and **1d** (Fig. 3) to those of the similar structures,

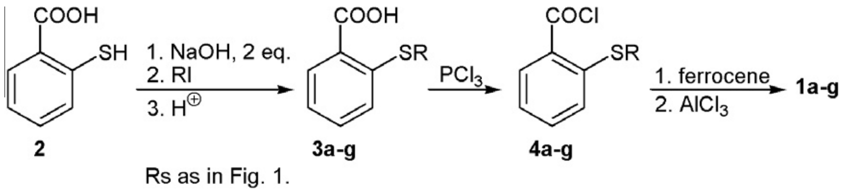

Scheme 1. Synthesis of (2-alkylthiobenzoyl)ferrocenes **1a–g**.

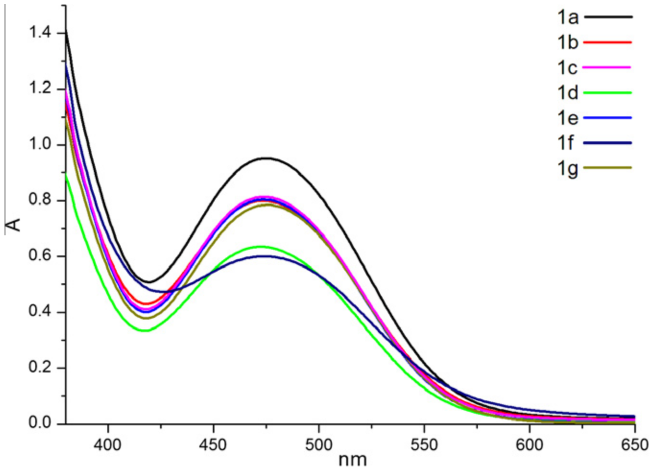

Fig. 2. UV spectra of compounds **1a**–**1g** in dichoromethane (1×10^{-3} mol L^{-1}).

the Cambridge Structural Database (CSD) [29] was used. We extracted 22 crystal structures [30–46] from CSD which comprise at least one structural fragment (benzoylferrocene moiety) shown in Fig. 4. The list of CSD refcodes and references of these 22 crystal structures are given in Supplementary material (Table 1S).

The cyclopentadienyl rings in **1a, 1b** and **1d** adopt a nearly eclipsed geometry. The values of the torsion angles C10–Cg1–Cg2–C1 (which relate the substituted C10 and corresponding, eclipsed C1 atoms through centroids of the Cp rings, Cg1 and Cg2) are 2.9, 9.0 and 15.7° in **1a**, **1b** and **1d**, respectively, indicating an increasing deviation from the regular eclipsed conformation in the same order. This is the major difference considering the geometry of the ferrocene units in the three derivatives. The same C10–Cg1–Cg2–C1 torsion angle was analyzed for 22 crystal structures extracted from CSD. Distribution of the torsion angle values is given in the Supplementary material (Fig. 1S) indicating the range from 0 to 16° as the most frequent.

The C–C bonds within the Cp rings are consistent; it should be noticed however, that in all three compounds the C–C bonds within the substituted rings, Cp1 (average values: 1.418, 1.421 and 1.418 Å in **1a**, **1b** and **1d**, respectively) are slightly longer than in the unsubstituted rings, Cp2 (average values: 1.408, 1.392 and 1.400 Å in **1a**, **1b** and **1d**, respectively). The longest bonds in Cp1 are C6–C10 and C9–C10 which are placed in the vicinity of the carbonyl substituent bonded to C10 atom (Fig. 3). The pairs of Cp1 and Cp2 rings show only small mutual tilting as evidenced from the corresponding Cp1/Cp2 dihedral angles which are all below 3.1°.

There is a very slight difference in the distances of the Fe atom from the least-square planes of the Cp rings and in each of the cases the metal is positioned closer to the substituted ring Cp1 for approximately 0.01 Å. The scatterplot in the Supplementary material (Fig. 2S) compares the distances between the Fe atom and the least-square planes of Cp1 and Cp2 in 22 extracted crystal structures. It can be noticed that in the majority of structures, this difference is below 0.015 Å and only in two cases exceeds the value of 0.02 Å.

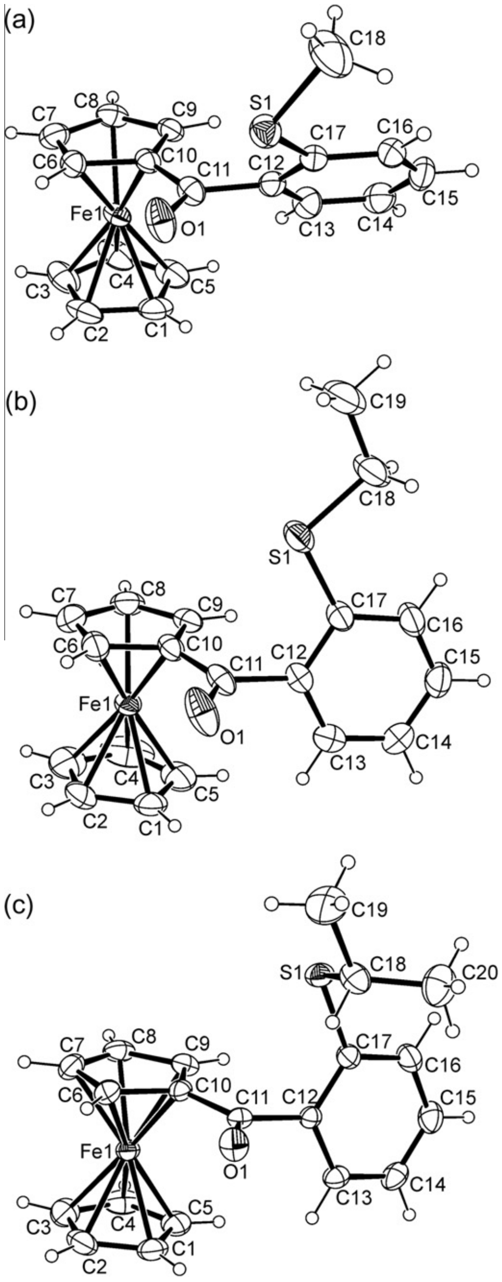

Fig. 3. Crystal structures and atom-numbering scheme of compounds **1a** (a), **1b** (b) and **1d** (c). Displacement ellipsoids are drawn at the 40% probability level.

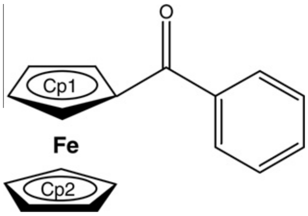

Fig. 4. Fragment used in CSD search.

Special attention was devoted to the spatial position of the carbonyl group with regard to the rest of molecule (in all analyzed crystal structures this group is bonded to the same structural fragments, ferrocene moiety and phenyl ring). In the present derivatives the carbonyl moiety, C11–O1, is almost coplanar with Cp1 ring. The angle between the vector coinciding the C11–O1 bond and the Cp1 plane is equal to 1.4°, 6.4° and 5.0° in **1a**, **1b** and **1d**, respectively. This coplanar position is supported by rather bent intramolecular C6–H…O1 contact which is present in all these compounds (Table 2). The angle between the carbonyl vector and the phenyl fragment is on the other hand much larger and equal to 48.1°, 76.0° and 77.0°. The scatterplot in Fig. 3S displays a disposition of this vector (V1) with regard to the corresponding Cp1 (Cp1/V1) and Ph (Ph/V1) planes in 22 similar crystal structures. It is evident that in almost all crystal structures the carbonyl moieties are preferable coplanar to Cp1 rings. The maximal deviations from the Cp1 planes are always below 20°, at the same time, the deviation angles from Ph rings can exceed 65°. The values corresponding to the three present derivatives, (also assigned in scatterplot), indicate that the deviations of the carbonyl groups from the Ph rings are larger in compounds **1b** and **1d** than in all other structures. The different behavior i.e. the better co-planarity of the carbonyl group with Ph ring instead of Cp1 is observed only in one crystal structure, RUVHEV [30]. This crystal structure however contains rather strong competing intramolecular hydrogen bond which engages the carbonyl to the neighboring hydroxyl group and probably influences its final position.

It should be also emphasized that in the present crystal structures C10–C11 bond which attaches the carbonyl moiety to Cp1 ring is always shorter in comparison to C11–C12 toward the Ph ring (Table 3). The same relation between the two bond lengths is also found in the 22 crystal structures extracted from CSD (Fig. 4S) with only one exception, the coordination polymer IKAZOJ [31]. The shorter length of the C10–C11 bond is probably a consequence of π-electron delocalization existing between the Cp1 ring and the carbonyl group. In addition to the previously mentioned intramolecular C–H…O interaction this delocalization can contribute to the coplanar arrangement of the two moieties.

The orientation of the phenyl rings with regard to the Cp1 could be considered as a main geometrical dissimilarity between the described (*S*-alkylbenzoyl)ferrocene derivatives. In compound **1a** which has the smallest, *S*-methyl, substituent the dihedral angle between the least-square planes of the Ph and Cp1 rings is 46.8(3)°. This is larger than found in two crystal structures describing unmodified Benzoylferrocene (ZZZHCY01 [32a] and ZZZHCY02 [32b]) where this angle is equal to 37.7° and 38.3°. In *S*-ethyl and *S*-isopropyl derivatives the Ph moiety becomes more perpendicularly positioned making the dihedral angles of 82.4(1)° and 80.2(2)°.

Table 3
Selected bond lengths (Å) and bond angles (°) in crystal structures of **1a**, **1b** and **1d**.

	1a	**1b**	**1d**
O1–C11	1.226(6)	1.226(3)	1.225(4)
C10–C11	1.485(10)	1.424(4)	1.468(5)
C11–C12	1.499(8)	1.514(4)	1.511(5)
S1–C17	1.766(6)	1.757(3)	1.781(4)
S1–C18	1.796(9)	1.807(3)	1.836(5)
C18–C19		1.470(6)	1.491(6)
C18–C20			1.528(6)
O1–C11–C10	119.7(6)	122.2(3)	122.8(4)
O1–C11–C12	119.9(6)	119.4(3)	119.5(4)
C6–C10–C11	107.9(6)	106.8(3)	107.9(5)
C9–C10–C11	129.1(7)	125.9(3)	126.1(4)
C11–C12–C13	121.3(5)	118.8(2)	120.3(5)
C11–C12–C17	119.1(5)	121.3(3)	120.9(4)
C17–S1–C18	103.0(4)	104.5(2)	101.3(4)

The three crystal structures lack in typical hydrogen bonding donors, thus, despite the presence of the carbonyl oxygen acceptor, the crystal packing is stabilized only by weak C–H…O, C–H…S and C–H…π interactions (Table 2S). The different types of C–H donors, Cp in **1a**, Cp and Ph in **1b** and Cp, Ph and alkyl in **1d** are engaged in interactions to carbonyl groups. The C–H…O interaction in **1a** and **1b** which can be considered as the shortest involve Cp hydrogens and connect the corresponding molecules into chains with clear directional preferences along the *c* and *b* axis, respectively. It is, however, interesting to point out to particular structural motif which seems to characterize each of these crystal structures. Namely, in the crystal arrangements of **1a, 1b** and **1d**, the Ph ring is positioned in a nearly perpendicular orientation to some of C–H groups from the neighboring Cp rings (see Fig. 5S in the Supplementary material). In that way the Ph ring acts as a π acceptor in the intermolecular C–H…π interactions to the neighboring Cp rings. The perpendicular distance of the H atom from the plane of the phenyl ring (H_{perp}…Ph) in these interactions is shorter than 3.05 Å what could be accepted as satisfactory for the existence of C–H…π interactions [**1a**: C6–H6…Ph^{i}, H_{perp}…Ph = 3.03 Å, (i) = $-x+1,\ y-1/2,\ -z+2$; **1b**: C8–H8…Ph^{i}, H_{perp}…Ph = 3.04 Å, and C4–H4…Ph^{i}, H_{perp}…Ph = 2.71 Å, (i) = $-x+1/2,\ -y+1/2,\ -z+1$; **1d**: C8–H8…Ph^{i}, H_{perp}…Ph = 2.92 Å, (i) = $-x+1,\ -y+2,\ -z$].

In the centrosymmetrical crystal structures **1b** and **1d** above described intermolecular C–H…π interactions relate the molecules into pairs, while in the non-centrosymmetrical structure **1a** the C–H…π interactions assemble the molecules into chain extended in *b* direction. The similar structural motif was also observed in several other crystal structures such as: TIDXOU [33], YARRUE [34], ZZZHCY01 [32a], ZZZHCY02 [32b], CIXNED [35] and COCKOV [36]. The **1a, 1b** and **1d** crystal structures are also stabilized by additional C–H…π interactions where C–H groups of the phenyl moieties interact with the cyclopentradienyl π system [**1a**: C16–H16…Cp1^{ii}, H_{perp}…Cp1 = 3.04 Å, (ii) = $-x,\ y+1/2,\ -z+2$; **1d**: C13–H13…Cp2^{ii}, H_{perp}…Cp2 = 2.88 Å, (ii) $-x+1,\ -y+1,\ -z$], as well as the C–H…π interactions where alkyl C–H groups interact with both type of π systems [**1a**: C18–H18a…Cp2^{iii}, H_{perp}…Cp2 = 2.78 Å, (iii) = $x-1,\ y,\ z+1$ and C18–H18c…Cp1^{ii}, H_{perp}…Cp1 = 2.50 Å; **1b**: C18–H18b…Cp2^{ii}, H_{perp}…Cp2 = 2.98 Å, (ii) = $x+1/2,\ -y+1/2,\ z+1/2$; **1d**: C20–H20c…Ph^{iii}, H_{perp}…Ph = 3.00 Å, (iii) = $-x+2,\ y+1/2,\ -z+1/2$ and C20–H20a…Cp2^{iv}, H_{perp}…Cp2 = 3.03 Å, (iv) = $x+1,\ -y+3/2,\ z+1/2$].

Table 2
Geometrical parameters for intra- and intermolecular C–H…A (A = O and S) interactions in crystal structures of **1a**, **1b** and **1d**. All H atoms are placed at geometrically calculated positions.

	D–H…A	D–H (Å)	H…A (Å)	D…A (Å)	D–H…A (°)	Symmetry codes
1a	C6–H6…O1	0.93	2.72	2.872(8)	89.6	x, y, z
	C4–H4…O1	0.93	2.60	3.190(8)	123.7	$x, y, z-1$
	C7–H7…O1	0.93	2.67	3.482(9)	146.1	$-x+1, y-1/2, -z+2$
	C5–H5…S1	0.93	3.13	3.859(7)	136.5	$x, y, z-1$
	C15–H15…S1	0.93	3.07	3.871(7)	145.5	$-x, y+1/2, -z+2$
1b	C6–H6…O1	0.93	2.83	2.883(3)	86.4	x, y, z
	C1–H1…O1	0.93	2.43	3.211(5)	141.4	$-x+1/2, y+1/2, -z+½$
	C13–H13…O1	0.93	2.61	3.498(4)	161.1	$-x+1/2, y+1/2, -z+½$
	C15–H15…S1	0.93	3.07	3.826(4)	139.3	$x, y+1, z$
1d	C6–H6…O1	0.93	2.87	2.978(6)	87.2	x, y, z
	C7–H7…O1	0.93	2.76	3.317(6)	119.6	$-x+1, y+1/2, -z+1/2$
	C15–H15…O1	0.96	2.79	3.298(6)	115.0	$x, -y+3/2, -1/2+z$
	C19–H19b…O1	0.93	2.76	3.669(7)	158.5	$x+1/2, y+1/2, -z+1/2$
	C4–H4…S1	0.93	3.07	3.994(6)	171.1	$-x+1, -y+2, -z$

Table 4
Electrochemical data of compounds **1a**–**g**.

Compounds	E_{pa} (mV)[a]	E_{pc} (mV)[a]	$E_{1/2}$ (mV)[b]	ΔE (mV)[c]
1a	383	310	346.5	73
1b	383	307	345	76
1c	383	309	346	74
1d	384	308	346	76
1e	380	306	343	74
1f	389	303	346	86
1g	383	311	347	72

[a] E_{pa} and E_{pc} anodic and cathodic peak potentials, respectively, at 100 mV s^{-1}.
[b] $E_{1/2} = (E_{pa} + E_{pc})/2$.
[c] $E = E_{pa} - E_{pc.}$

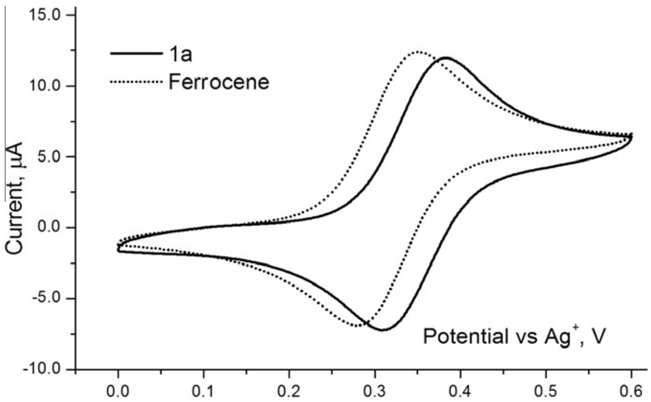

Fig. 5. Cyclovoltammograms of compound **1a** and ferrocene at Pt disc in 0.1 M $LiClO_4$ in acetonitrile at $v = 0.1$ V/s.

3.4. Electrochemistry

Cyclic voltammetry in acetonitrile containing 0.1 mol/L lithium perchlorate as a supporting electrolyte has been used for the evaluation of electrochemical properties of the synthesized compounds **1a–g**. All ketones exhibit a reversible one-electron redox couple at almost the same potential. Oxidation waves appear at 380–389 mV, whereas the reduction ones at 303–311 mV, and we attributed them to the oxidation of the ferrocene unit by the forward potential sweep, and reduction of the obtained ferricinium ion at the beck potential sweep. These potentials are slightly more positive than that of the unsubstituted ferrocene, as a consequence of the presence of an electron-withdrawing acyl group (see Table 4).

As the representative example we give the voltammogram of compound **1e** (solid line, Fig. 5) together with the voltamogram of ferrocene (dashed line, Fig. 5). The difference between anodic and cathodic peak potentials is close to the theoretical value and independent of the scan rate *v*. Both, anodic and cathodic peak currents are proportional to the square root of the scan rate (see Fig. 6S in the Supplementary material), and their ratio is independent of the scan rate, indicating a diffusion-controlled process.

4. Conclusions

In conclusion, we showed that (2-alkylthiobenzoyl)ferrocenes can be synthesized by a one-pot acylation procedure from the corresponding 2-alkylthiobenzoic acids, phosphorus trichloride and ferrocene without isolation of the intermediate acid chlorides. The seven new sulfur containing ketones – ferrocene derivatives – were well characterized by spectral data (IR, NMR and UV). As the cyclovoltammetric measurements showed, these ketones exhibit a reversible one-electron redox couple at almost the same potential.

Three new crystal structures are characterized by single-crystal X-ray analysis and their geometrical parameters are compared to additional 22 crystal structures of benzoylferrocenes extracted from Cambridge Structural Database. Special attention was devoted to spatial position of the carbonyl group with regard to the rest of the molecule (ferrocene moiety and phenyl ring). It was found that in almost all crystal structures the carbonyl moiety is preferable coplanar to Cp1 ring. Except in one case, the maximal deviations of the C–O (carbonyl) vector from the Cp1 plane are always below 20°, at the same time, the deviation angles from Ph rings are above 20° and can exceed 65°. It should be also emphasized that in all crystal structures the C–C bond which attaches the carbonyl moiety to Cp1 ring is always shorter (more than 0.03 Å in average) in comparison to C–C bond toward the Ph ring. Analysis of intermolecular interactions shown that Cp and Ph rings from benzoylferrocene can act as a π acceptors in the C–H…π interactions.

Acknowledgements

This work was supported by the Ministry of Science and Technological Development of the Republic of Serbia (Grants 142042 and 142010).

Appendix A. Supplementary data

CCDC 771043, 771044 and 771045 contain the supplementary crystallographic data for **1a**, **1b** and **1d**. These data can be obtained free of charge via http://www.ccdc.cam.ac.uk/conts/retrieving.html, or from the Cambridge Crystallographic Data Centre, 12 Union Road, Cam-bridge CB2 1EZ, UK; fax: (+44) 1223–336-033; or e-mail: deposit@ccdc.cam.ac.uk. Supplementary data associated with this article can be found, in the online version, at doi:10.1016/j.poly.2010.04.034.

References

[1] A. Togni, T. Hayashi, Ferrocenes: Homogenous Catalysis, Organic Synthesis, Material Science, VCH, Weinheim, Germany, 1995.
[2] A. Togni, R.L. Haltermann, Metallocenes, Wiley-VCH, Weinheim, Germany, 1998.
[3] B. Loev, M. Flores, J. Org. Chem. 26 (1961) 3595.
[4] F.D. Popp, S. Roth, J. Kirby, J. Med. Chem. 6 (1963) 83.
[5] C. Biot, G. Glorian, L.A. Maciejewski, J.S. Brocard, J. Med. Chem. 40 (1997) 3715.
[6] D. Osella, M. Ferrali, P. Zanello, F. Laschi, M. Fontani, C. Nervi, G. Cavigiolio, Inorg. Chim. Acta 306 (2000) 42.
[7] G. Jaouen, S. Top, A. Vessières, R. Alberto, J. Organomet. Chem. 600 (2000) 23.
[8] D.R. van Staveren, N. Metzler-Nolte, Chem. Rev. 104 (2004) 5931.
[9] E.W. Neuse, J. Inorg. Organomet. Polym. 15 (2005) 3.
[10] C.S. Allardyce, A. Dorcier, C. Scolaro, P.J. Dyson, Appl. Organomet. Chem. 19 (2005) 1.
[11] G. Jaouen, W. Beck, M.J. McGlinchey, in: G. Jaouen (Ed.), Bioorganometallics: Biomolecules, Labeling, Medicine, Wiley-VCH, Weinheim, 2006.
[12] M.F.R. Fouda, M.M. Abd-Elzaher, R.A. Abdelsamaia, A.A. Labib, Appl. Organomet. Chem. 21 (2007) 613.
[13] O. Payen, S. Top, A. Vessières, E. Brulé, M.-A. Plamont, M.J. McGlinchey, H. Müller-Bunz, G. Jaouen, J. Med. Chem. 51 (2008) 1791.
[14] I. Damljanović, M. Vukićević, N. Radulović, R. Palić, E. Ellmerer, Z. Ratković, M.D. Joksović, R.D. Vukićević, Bioorg. Med. Chem. Lett. 19 (2009) 1093.
[15] R.B. Woodward, M. Rosenblum, M. Whiting, J. Org. Chem. 74 (1952) 3458.
[16] R.D. Vukićević, M. Vukićević, Z. Ratković, S. Konstantinović, Synlett (1998) 1329.
[17] M.D. Vukićević, Z.R. Ratković, A.V. Teodorović, G.S. Stojanović, R.D. Vukićević, Tetrahedron 58 (2002) 9001.
[18] R.D. Vukićević, D. Ilić, Z. Ratković, M. Vukićević, Monats. Chem. 132 (2001) 625.
[19] D. Ilić, I. Damljanović, D. Stevanović, M. Vukićević, N. Radulović, V. Kahlenberg, G. Laus, R.D. Vukićević, Polyhedron 29 (2010) 1863.
[20] R.J. Irving, W.C. Fernelius, J. Phys. Chem. 60 (1956) 1427.
[21] Enraf-Nonius CAD4 Software, Version 5.0, Enraf-Nonius, Delft, The Netherlands, 1989.
[22] CAD-4 Express Software, Enraf-Nonius, Delft, The Netherlands, 1994.

[23] (a) G.M. Sheldrick, SHELXS97. Program for the Solution of Crystal Structures, University of Göttingen, Germany, 1997;
(b) G.M. Sheldrick, SHELXS97. Program for the Refinement of Crystal Structures, University of Göttingen, Germany, 1997.
[24] L.J. Farrugia, J. Appl. Crystallogr. 32 (1999) 837.
[25] (a) A.L. Spek, Acta Crystallogr. A46 (1990) C34;
(b) A.L. Spek, PLATON, A Multipurpose: Crystallographic Tool, Utrecht University, Utrecht, The Netherlands, 1998.
[26] M. Nardelli, PARST, J. Appl. Crystallogr. 28 (1995) 659.
[27] L.J. Farrugia, ORTEPIII for Windows – J. Appl. Crystallogr. 30 (1997) 565.
[28] G. Eminović, M. Vukićević, Z. Ratković, D. Ilić, R.D. Vukićević, Synlett (2003) 2416.
[29] F.H. Allen, Acta Crystallogr. B58 (2002) 380.
[30] C. Glidewell, S.Z. Ahmed, J.F. Gallagher, G. Ferguson, Acta Crystallogr. C53 (1997) 1775.
[31] G. Li, H. Hou, L. Li, X. Meng, Y. Fan, Y. Zhu, Inorg. Chem. 42 (2003) 4995.
[32] (a) I.R. Butler, W.R. Cullen, S.J. Rettig, J. Trotter, Acta Crystallogr. C44 (1988) 1666;
(b) J.C. Barnes, W. Bell, C. Glidewell, R.A. Howie, J. Organomet. Chem. 385 (1990) 369.
[33] G. Li, Z.-F. Li, J.-X. Wu, L. Zhu, H.-W. Hou, Chin. J. Inorg. Chem. 23 (2007) 975.
[34] T.V. Baukova, L.G. Kuzmina, N.V. Dvortsova, Russ. J. Inorg. Chem. 37 (1992) 1497.
[35] G. Li, Z.-F. Li, J.-X. Wu, C. Yue, H.-W. Hou, J. Coord. Chem. 61 (2008) 464.
[36] G. Li, C. Yue, J. Wu, L. Wang, H. Hou, React. Inorg., Met.-Org., Nano-Met. Chem. 37 (2007) 267.
[37] S.Z. Ahmed, G. Ferguson, C. Glidewell, J. Organomet. Chem. 585 (1999) 331.
[38] K. Heinze, M. Schlenker, Eur. J. Inorg. Chem. (2004) 2974.
[39] W. Figueroa, M. Fuentealba, C. Manzur, A.I. Vega, D. Carrillo, J.R. Hamon, C.R. Chim. 8 (2005) 1268.
[40] J.F. Gallagher, G. Ferguson, S.Z. Ahmed, C. Glidewell, A. Lewis, Acta Crystallogr. C53 (1997) 1772.
[41] M. Erben, A. Ruzicka, J. Vinklarek, V. Stava, D. Vesely, Acta Crystallogr. E63 (2007) m3067.
[42] A.C. Benyei, C. Glidewell, P. Lightfoot, B.J.L. Royles, D.M. Smith, J. Organomet. Chem. 539 (1997) 177.
[43] Y.J. Wu, X.L. Cui, Y.H. Liu, H.Z. Yuan, X.A. Mao, J. Organomet. Chem. 543 (1997) 63.
[44] K. Heinze, M. Beckmann, J. Organomet. Chem. 691 (2006) 5576.
[45] Y.Y. Dou, Y.F. Xie, L.F. Tang, Appl. Organomet. Chem. 22 (2008) 25.
[46] G. Calvarin, D. Weigel, Acta Crystallogr. B27 (1971) 1253.